J Radioanal Nucl Chem (2016) 308:213–220
DOI 10.1007/s10967-015-4315-y

Study on adsorption characteristics of uranyl ions from aqueous solutions using zirconium hydroxide

Hongxue Liu[1] · Rui Wang[1] · Heng Jiang[1] · Hong Gong[1] · Xiaomeng Wu[1]

Received: 27 May 2015 / Published online: 25 July 2015

Abstract The removal of uranyl ions from aqueous solutions using $Zr(OH)_4 \cdot 3.35H_2O$ (ZH) as adsorbent was investigated using a batch adsorption technique. The maximum removal rate was found as 451.7 mg $UO_2^{2+} \cdot g^{-1}$ ZH. The adsorption capacity and adsorption rate of the calcinated products gradually decreases with increasing calcination temperature. The hydroxyl groups in the zirconium hydroxide play an important role for the adsorption uranyl ions, which agree well with the thermogravimetric analysis of zirconium hydroxide for completely dehydration at 700 °C. The observed data shows that the adsorption process is dependent on surface complexation mechanism.

Keywords Zirconium hydroxide · Calcinated product · Uranyl ions · Adsorption

Introduction

Uranium is a chemically toxic and slightly radioactive heavy metal used in nuclear industry. The environmental pollution is the most serious problem which should be taken into consideration for increasing radioactive contamination. Like many other heavy metals such as chromium, lead, mercury and nickel, uranium and its compounds are highly poisonous substances. Uranium can enter the human body through respiration or through contact with an open wounds and its radioactivity also poses increased risks of lung cancer and bone cancer [1–4]. Thus, removal of uranyl ions from wastewater should be concerned because of the significance of potential environmental hazards.

Various methods have been proposed to remove uranyl ions from wastewater, such as chemical precipitation [5], solvent extraction [6, 7], ion exchange [8, 9] and adsorption [10–24]. Adsorption is a desirable method due to its high efficiency, economical, eco-friendly operation.

In recent years, numerous studies have been conducted to remove uranyl ions from aqueous solutions using various adsorbents, such as zeolites [11, 12], clays [13], biological adsorbents [14, 15], chemically modified adsorbents [16–19], and polymeric adsorbents [20–24]. However, these adsorbents suffer from one or more drawbacks. Chemically modified adsorbents using different organic compounds generate useless substances which are harmful to the environment. Polymeric adsorbents suffer from high cost. The adsorption capacity and adsorption rate of zeolites, clays and biological adsorbents are low. The development of low cost, low-pollution, and efficient adsorbent for removing uranyl ions from wastewater is highly desired. It has been reported that zirconium hydroxide is effective for the adsorption of phosphate [25], chromium (VI) [26], H_2S [27], fluoride [28], SO_2 [29] and NH_3 [30]. As far as we known, no study has been done for removing uranyl ions from aqueous solution using zirconium hydroxide as adsorbent. Therefore, the adsorption behavior of uranyl ions on zirconium hydroxide, which is high adsorption capacity, green and environmentally friendly inorganic adsorbent, is investigated in this study.

✉ Heng Jiang
hjiang78@hotmail.com

[1] School of Chemistry and Materials Science, Liaoning Shihua University, Fushun 113001, China

Experimental

Materials

KOH, NaOH, HNO_3 and Arsenazo III used in these studies were analytical purity. Doubly distilled water was used in all experiments. Chemical pure grade of zirconium hydroxide $Zr(OH)_4{\cdot}3.35H_2O$, hereinafter referred to as ZH) was purchased from Sinopharm Chemical Reagent Co., Ltd as a dry powder and used without further purification. The formulation of ZH was calculated as $Zr(OH)_4{\cdot}3.35H_2O$ based on the thermogravimetric analysis.

Characterization

Thermogravimetric analysis were carried out under air flow (20 mL min^{-1}) at a heating rate of 20 K min^{-1}, from 30 to 800 °C, in a Pyris 1 TGA (Perkin–Elmer).

FT-IR spectra were recorded on a Spectrum GX FT-IR spectrophotometer (Perkin Elmer) with samples as KBr pellets in the 4000–400 cm^{-1} region.

Adsorption studies

ZH were annealed in air at 100, 200, 300, 400, 500, 600, and 700 °C for 3 h at each temperature, which were refered to as ZH-100, ZH-200, ZH-300, ZH-400, ZH-500, ZH-600 and ZH-700, respectively. After naturally cooled down to room temperature, the corresponding calcinated product was used as adsorbent for investigating the removal efficiency for uranyl ions in aqueous solutions.

The pH of the solution was adjusted by adding a small amount of 0.1 mol L^{-1} HNO_3 or 0.1 mol L^{-1} KOH solutions. In a typical experiment, 0.01 g of ZH was added into 24 mL uranyl ions solution (1.0 mmol L^{-1}) in a flask and stirred at 30 °C for 60 min. Then, the suspension was centrifuged and 0.5 mL supernatant was removed for uranyl ions determination. The quantitative determination of uranyl ions was performed by visible spectrophotometer using Arsenazo III as a chromogenic agent at a wavelength of 652 nm [31]. All the experiments were performed in triplicate. The total relative standard deviation was controlled within ±5 %.

The adsorption rate ($R\%$) and the adsorption capacity (q_e) are calculated by Eqs. (1) and (2):

$$R\% = \frac{C_0 - C_e}{C_0} \times 100\ \% \tag{1}$$

$$q_e = \frac{C_0 - C_e}{m} \times V, \tag{2}$$

where C_0 and C_e (mol L^{-1}) are the initial and the equilibrium concentrations of uranyl ions, respectively, V (L) is volume of the uranyl ions solution, m (g) is the weight of the adsorbents.

The adsorption isotherm and kinetics models

The isotherm experiments were performed using 0.25, 0.5, 0.75, 1.0 and 1.25 mmol L^{-1} of uranyl ions. For kinetic studies, three different initial concentrations of uranyl ions (0.75, 1.0 and 1.25 mmol L^{-1}) were used, and the contacting time was 1, 3, 5, 10, 15, 20, 25, 30, 40, 60 and 120 min, respectively. The equilibrium time was reached within 60 min.

The Freundlich and Langmuir isotherms were used to describe adsorption equilibrium [32], which is expressed as Eqs. (3) and (4), respectively.

$$\frac{C_e}{q_e} = \frac{1}{q_0 K_L} + \frac{C_e}{q_0} \tag{3}$$

$$\log q_e = \log K_F + \frac{1}{n} \log C_e, \tag{4}$$

where, q_0 (mg g^{-1}) is the Langmiur monolayer adsorption capacity and K_L (L g^{-1}) is the Langmuir constant. K_F (mg g^{-1}) and n are the Freundlich constant, which represent the adsorption capacity and adsorption intensity, respectively. q_e (mg g^{-1}) is the amount of solute adsorbed at equilibrium. C_e (mg L^{-1}) is the equilibrium concentration.

The pseudo-first-order kinetic model and pseudo-second-order kinetic model [33] were employed here to describe the kinetic characteristic of uranyl ions adsorbed by ZH.

The pseudo-first-order kinetic model is represented as Eq. (5):

$$\log(q_e - q_t) = \log q_e - \frac{k_1}{2.303} \times t. \tag{5}$$

The pseudo second-order kinetic model can be expressed as Eq. (6):

$$\frac{t}{q_t} = \frac{1}{k_2 q_e^2} + \frac{t}{q_t}. \tag{6}$$

In the models above, k_1 (min^{-1}) and k_2 (g mg^{-1} min^{-1}) denote the adsorption rate constants respectively; q_t (mg g^{-1}) is the adsorption capacity at time t.

Desorption experiments

0.01 g of ZH was stirred with 24 mL of uranyl ions solution (pH 5.0) at 30 °C for 60 min, then centrifuged for solid–liquid separation and the supernatant was removed for uranyl ions measurement. Subsequently, 24 mL of 0.01 mol L^{-1} HNO_3 eluting agent was added, followed by 120 min stirring at 30 °C. Finally, the uranyl ions

concentration in the desorption eluents was determined, and desorption efficiency was calculated. Desorption efficiency is determined by use of Eq. (7):

$$\text{Desorption } (\%) = \frac{\text{Amount of uranyl ions desorbed}}{\text{Amount of uranyl ions adsorbed}} \times 100\ \% \quad (7)$$

The solid was washed with water. The as-collected ZH was used for the sorption of uranyl ions in a second time as described above. According to this process, the adsorption/desorption process was repeated for six times.

Results and discussion

Adsorption mechanism

ZH calcinated at different temperature for 3 h were used as adsorbent for the removal of uranyl ions from aqueous solution. The adsorption behaviors are shown in Fig. 1. ZH exhibits the highest adsorption efficiency. As the increasing of calcination temperature, the adsorption capacity and adsorption rate of ZH-100 to ZH-700 gradually decrease. The calcinated product at 700 °C loses the adsorption capacity completely. The possible reason may be that the surface hydroxyl groups are lost due to the dehydration at high calcination temperature.

The formulation of ZH can be calculated as $Zr(OH)_4 \cdot 3.35H_2O$ according to the dehydration weight loss of 43.9 % at 700 °C (Fig. 2). It can be seen from Fig. 2 that the coordinated H_2O and hydroxyl groups are lost simultaneously. The maximum weight loss rate occurs at about 104 °C, indicating that the coordinated H_2O was completely lost and small amount of hydroxyl groups was also lost. The dehydration occurs continuously over the whole range of temperature 150–700 °C. The completely dehydration resulting the formation of ZrO_2 is observed at about 700 °C. According to the experimental results of Fig. 1, it is obvious that the hydroxyl groups in the ZH play an important role for the removal of uranyl ions from aqueous solutions.

The structure of ZH is complex because it is a thermally unstable substance in the form of amorphous state. One possible structural model of ZH may be an oligomer of four "cyclic tetramers" as shown in Fig. 3. The zirconium atoms are linked by double hydroxyl bridges. The tetramer unit has 16 zirconium atoms, 12 terminal hydroxyl groups, and 48 bridging OH groups [34].

Small amount of hydroxyl groups are still presents in the calcinated poroducts at 400–600 °C (Fig. 2), accordingly, the calcinated products exhibit somewhat adsorption capacity for the uranyl ions (Fig. 1). Therefore, it is reasonable to infer that uranyl ions are adsorbed on the surface of ZH via surface complexation with the oxygen atom in the surface hydroxyl groups rather than electrostatic attraction [36]. Figure 4 shows the schematic representation of the proposed adsorption mechanism. The dominated U(VI) specie is UO_2^{2+} at pH <5.0 ($\sum U = 3.7 \times 10^{-5}$ - mol L^{-1}) [37]. The presence of hydroxyl groups on the surface of ZH assures the capture of UO_2^{2+} by surface complexation mechanism. The pH value of the uranyl ions solution before and after adsorption is 5.0 and 4.88 respectively, indicating that H^+ in the surface hydroxyl groups of ZH is replaced by UO_2^{2+} via surface complexation.

Maximum adsorption capacity (q_{max}) is an important parameter in studying the efficiency of adsorbents. In comparison with other adsorbents listed in Table 1, the

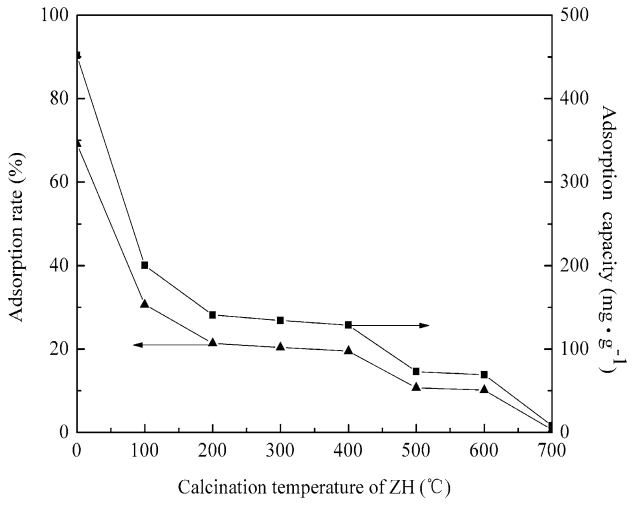

Fig. 1 Adsorption behaviours of ZH and its calcinated products (adsorbent dosage 0.01 g, initial concentration 1.0 mmol L^{-1}, contacting time 60 min, T 30 °C and pH 5.0)

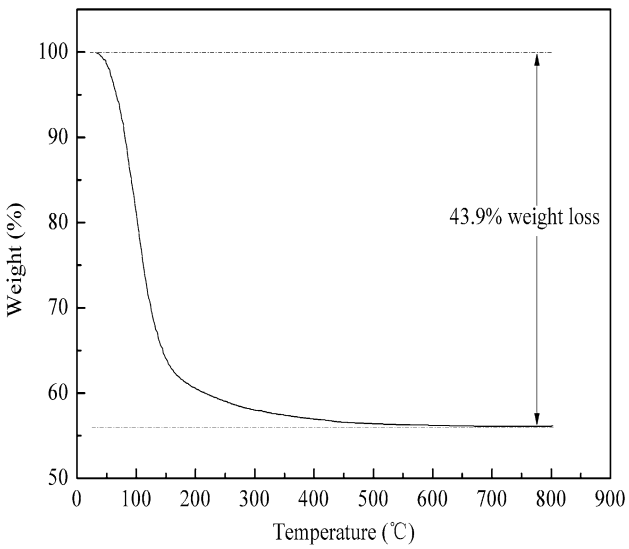

Fig. 2 The TG curve of the ZH

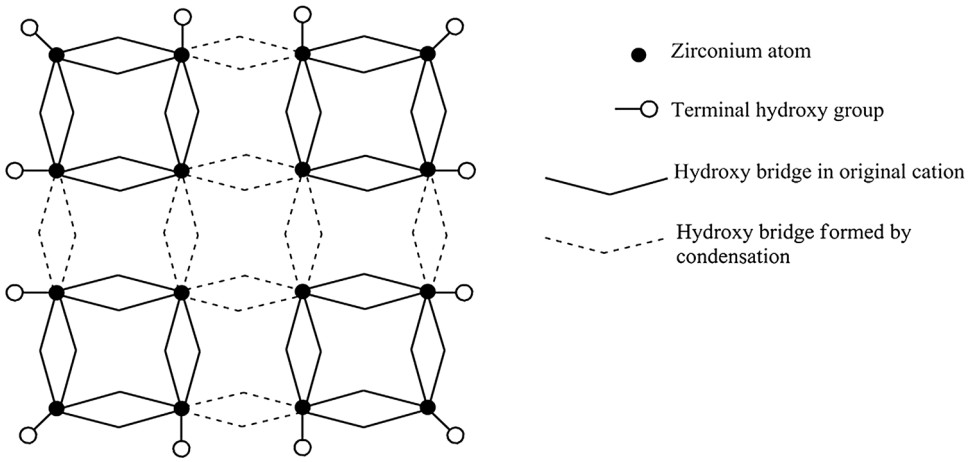

Fig. 3 Schematic diagram illustrating the structural model of ZH proposed by Southon et al. [35]

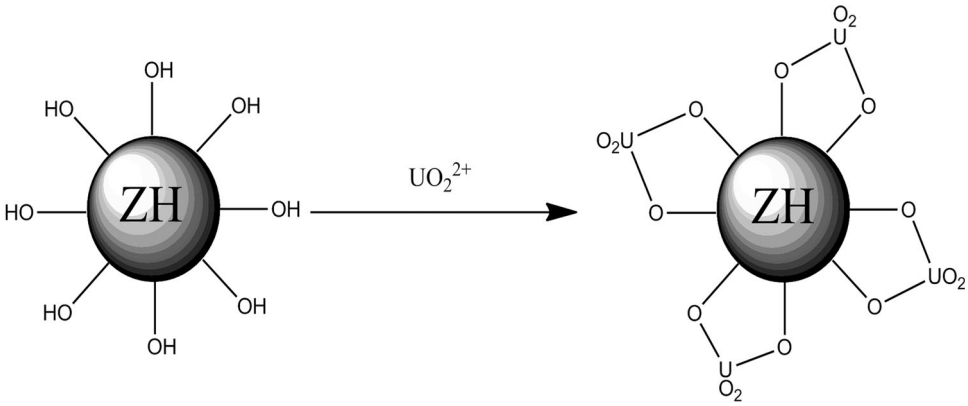

Fig. 4 The proposed schematic diagram of adsorption mechanism of uranyl ion by ZH

Table 1 Comparison of the q_{max} for different adsorbents

Adsorbents	Conditions	q_{max} (mg g^{-1})	Reference
Zeolite	Ph 6.0 $T = 293$ K	11.1	[11]
Humic acid-immobilized zirconium-pillared clay	pH 6.0 $T = 303$ K	132.7	[13]
Natural diatomite	pH 5 $T = 294$ K	6.1	[38]
Fe_3O_4@SiO_2	pH 6.0 $T = 298$ K	52	[39]
TiO_2	pH 4.5 $T = 318$ K	36.1	[40]
Geothite	pH 5.0 $T = 298$ K	28.2	[41]
Nano alumina	pH 5.0 $T = 298$ K	151.5	[41]
Graphene oxide/polypyrrole	pH 5.0 $T = 298$ K	147.1	[42]
Amidoxime modified Fe_3O_4@SiO_2	pH 5.0 $T = 298$ K	105	[43]
Cyclodextrin-modified graphene oxide nanosheets	pH 5.0 $T = 288$ K	97.3	[44]
Functionalized graphene oxide	pH 4.0 $T = 293$ K	138.9	[45]
Fe/Fe_3C@porous carbon sheets	pH 4 $T = 298$ K	About 2300	[46]
Poly(amidoxime)-reduced graphene oxide	pH 4.0 $T = 293$ K	872	[47]
ZH	pH 5.0 $T = 303$ K	451.7	This work

value of q_{max} for ZH removing uranyl ions was approximately 451.7 mg $UO_2^{2+}{\cdot}g^{-1}$ ZH. The comparison shows that the ZH exhibited markedly larger capacity for uranyl ions adsorption than most adsorbents.

FT-IR analysis

FT-IR spectra of the uranyl nitrate, ZH before and after uranyl ions adsorption are analyzed in order to further

illustrate the proposed adsorption mechanism. In Fig. 5a, strong peaks at 907 and 952 cm^{-1} in the uranyl nitrate spectra are assigned to the antisymmetrical and symmetrical vibrations of UO_2 group, respectively. The peaks at 1022, 1275 and 1531 cm^{-1} in the spectra are assigned to NO_2 out of plane vibration, NO and NO_2 stretching vibrations, respectively [48]. Compared Fig. 5b with 5c, no nitrate or nitrato adsorption peaks are observed in the FT-IR spectra after uranyl ions adsorption, suggesting that they are not participated in uranyl ions adsorption process. The new peaks at 903 and 1390 cm^{-1} are due to the vibration of UO_2 group appeared in Fig. 5c. The O–H stretching vibration bands have shifted from 3429 to 3397 cm^{-1} probably due to the binding of uranyl ions to hydroxyl groups [49, 50]. The above FT-IR analysis results show that uranyl ions may be adsorbed by complexation with surface hydroxyl groups on the ZH.

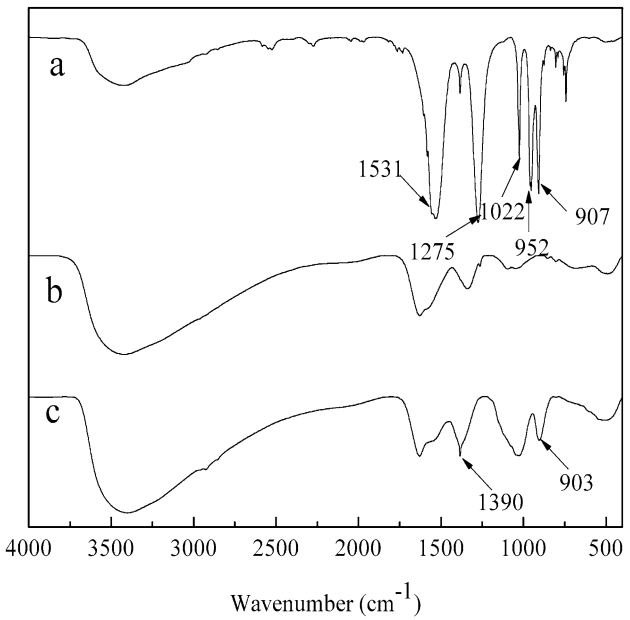

Fig. 5 A comparison of FT-IR spectra of **a** uranyl nitrate, ZH **b** before and **c** after uranyl ions adsorption

Figure 6 shows FT-IR spectra of the ZH before and after adsorption of uranyl ions at different calcination temperature. Compared Fig. 6b with Fig. 6a, there are vibration peaks of UO_2 group at 903 and 1390 cm^{-1} in the spectra of the ZH products calcined at all temperature except 700 °C. The decreasing intensity at 903 cm^{-1} in the spectra from ZH-100 to ZH-600 indicates that the calcinated products have less hydroxyl groups than calcinated ZH at higher temperature. The result agrees well with the results of adsorption experiments. It is further confirmed that the hydroxyl groups of ZH plays an important role in the adsorption of uranyl ions.

Adsorption isotherm and kinetics of uranyl ions adsorption on ZH

Figure 7 presents linearized Langmuir and Freundlich isotherms of ZH adsorption uranyl ions at 30 °C. This demonstrates that the adsorption of uranyl ions on ZH is best described by Langmuir isotherm and the adsorption is a homogeneous surface by monolayer adsorption. Moreover, the calculated value of q_{max} (448.4 mg $UO_2^{2+}{\cdot}g^{-1}$ ZH) from Langumir equation is relatively close to the experimental value of 451.7 mg $UO_2^{2+}{\cdot}g^{-1}$ ZH.

The adsorption kinetic parameters are calculated from the slopes and intercepts of the fitted curves in Fig. 8, and all the kinetic data are listed in Table 2, the pseudo-second-order kinetic model is most suited to describe the

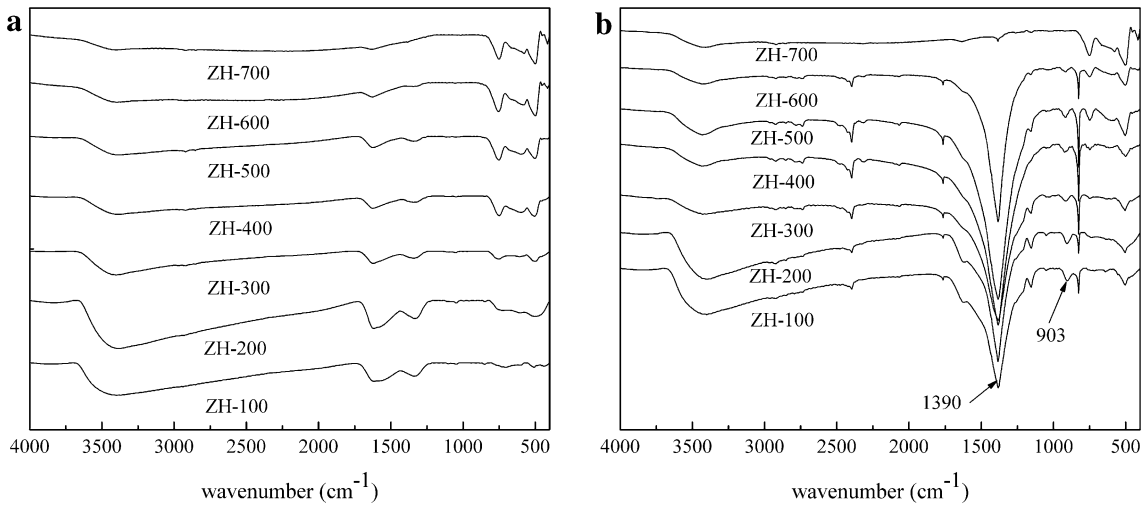

Fig. 6 A comparison of FT-IR spectra of the ZH calcinated products **a** before and **b** after adsorption of uranyl ions

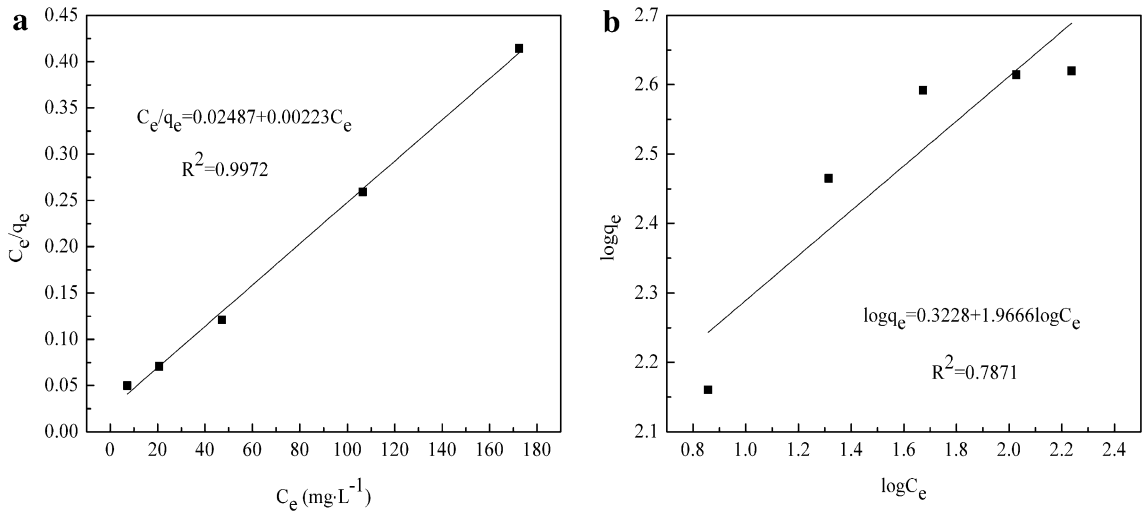

Fig. 7 Adsorption isotherm of **a** Langmuir and **b** Freundlich

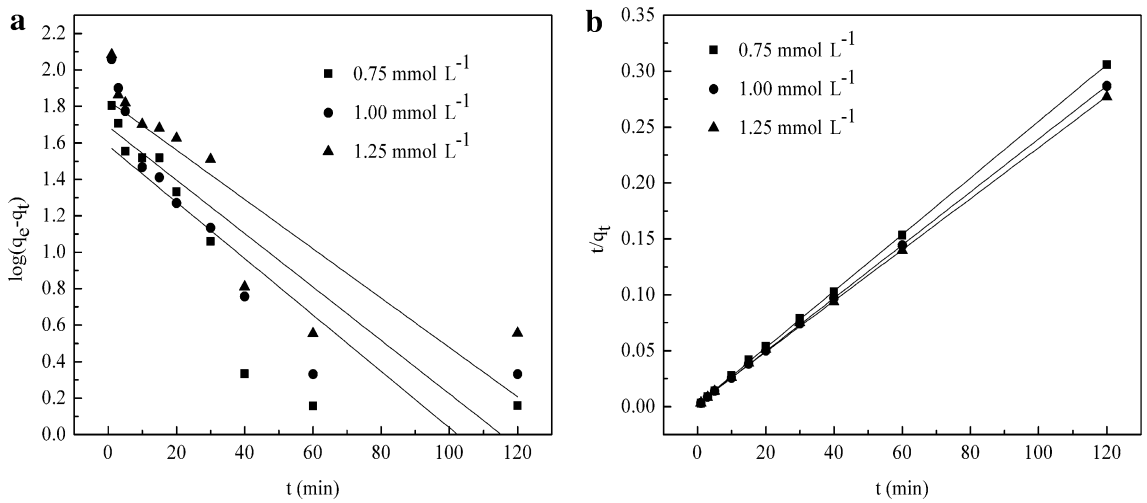

Fig. 8 **a** Pseudo-first-order and **b** pseudo-second-order plots for the adsorption of uranyl ions

adsorption process of uranyl ions by ZH. The results indicate that adsorption process involves chemical reaction between the uranyl ions and the surface hydroxyl groups of the ZH adsorbent.

Desorption and reusability

The adsorbed uranyl ions could be desorbed using 0.01 mol L^{-1} HNO_3 within 120 min and the desorption efficiency is higher than 90 %. The desorption efficiency in 0.001 mol L^{-1} HNO_3 decreased to 60 %. There is no desorption when the pH is greater than 5. The desorption experiment results indicate ZH can be regenerated very well with 0.01 mol L^{-1} HNO_3 solution. The reusability of ZH for uranyl ions adsorption is tested through many cycles of adsorption/desorption processes. It can be seen from Fig. 9 that the recycling is valid for at last six times. This result suggests that the adsorption of UO_2^{2+} on ZH is highly reversible.

Conclusions

Zirconium hydroxide (ZH) exhibits very high adsorption capacity for the removal of uranyl ions from aqueous solutions at pH 5.0. The role of surface hydroxyl group was demonstrated by investigating the adsorption efficiency of different calcinated products at different temperature. FT-IR analysis results show that the surface hydroxyl groups of ZH may coordinate with uranyl ions. Experimental kinetic data indicate that the adsorption process follow the pseudo-second-order kinetic model, revealing that uranyl ions

Table 2 Kinetic data for the adsorption of uranyl ions onto ZH

C_0 (mmol L^{-1})	Pseudo-first-order			Pseudo-second-order		
	$k_1 \times 10^{-2}$	q_e (mg g^{-1})	R^2	$k_2 \times 10^{-3}$	q_e (mg g^{-1})	R^2
0.75	3.56	38.4	0.7177	3.22	395.3	0.9999
1.00	3.38	48.9	0.7377	2.80	421.9	0.9999
1.25	3.11	67.9	0.7405	1.69	436.7	0.9995

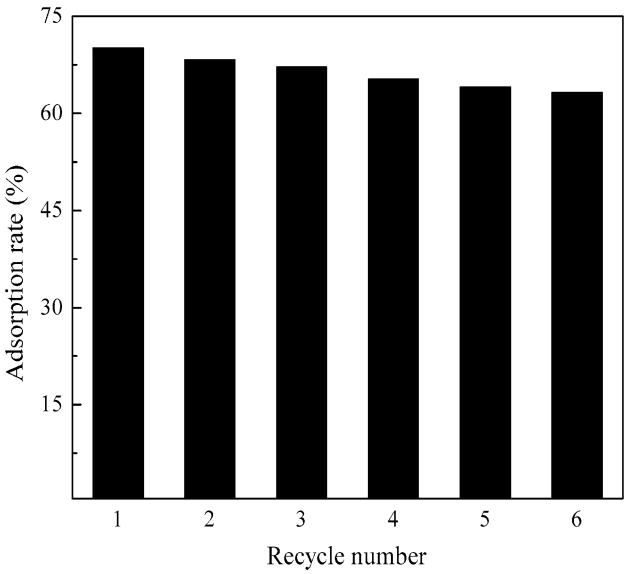

Fig. 9 Recycling of uranyl ions adsorption onto ZH

adsorption on ZH may be based on chemical adsorption. The experimental results indicated that ZH could be considered as effective inorganic adsorbents for the removal of uranyl ions from aqueous solutions.

Acknowledgments This work was financially supported by Scientific Research Project (No. L2012134) of Educational Department of Liaoning Province.

References

1. Preetha CR, Gladis JM, Rao TP (2006) Removal of toxic uranium from synthetic nuclear power reactor effluents using uranyl ion imprinted polymer particles. Environ Sci Technol 40:3070–3074
2. Yakout SM, Rizk MA (2015) Adsorption of uranium by low-cost adsorbent derived from agricultural wastes in multi-component system. Desalin Water Treat 53:1917–1922
3. Majdan M, Pikus S, Gajowiak A, Sternik D, Zięba E (2010) Uranium sorption on bentonite modified by octadecyltrimethylammonium bromide. J Hazard Mater 184:662–670
4. Jin JY, Huang X, Zhou LM, Peng J, Wang Y (2015) In situ preparation of magnetic chitosan resins functionalized with triethylene-tetramine for the adsorption of uranyl(II) ions. J Radioanal Nucl Chem 303:797–806
5. Kanematsu M, Perdrial N, Um W, Chorover J, O'Day PA (2014) Influence of phosphate and silica on U(VI) precipitation from acidic and neutralized wastewaters. Environ Sci Technol 48:6097–6106
6. Fan FL, Bai J, Fan FY, Yin XJ, Wang Y, Tian W, Wu XL, Qin Z (2014) Solvent extraction of uranium from aqueous solutions by α-benzoinoxime. J Radioanal Nucl Chem 300:1039–1043
7. Beltrami D, Cote G, Mokhtari H, Courtaud B, Moyer BA, Chagnes A (2014) Recovery of uranium from wet phosphoric acid by solvent extraction processes. Chem Rev 114:12002–12023
8. Ladeira ACQ, Morais CA (2005) Uranium recovery from industrial effluent by ion exchange—column experiments. Miner Eng 18:1337–1340
9. Banerjee C, Dudwadkar N, Tripathi SC, Gandhi PM, Grover V, Kaushik CP, Tyagi AK (2014) Nano-cerium vanadate: a novel inorganic ion exchanger for removal of americium and uranium from simulated aqueous nuclear waste. J Hazard Mater 280:63–70
10. Al-Hobaib AS, Al-Suhybani AA (2014) Removal of uranyl ions from aqueous solutions using barium titanate. J Radioanal Nucl Chem 299:559–567
11. Zou WH, Bai HJ, Zhao L, Li K, Han RP (2011) Characterization and properties of zeolite as adsorbent for removal of uranium(VI) from solution in fixed bed column. J Radioanal Nucl Chem 288:779–788
12. Abdi MR, Shakur HR, Saraee KRE, Sadeghi M (2014) Effective removal of uranium ions from drinking water using CuO/X zeolite based nanocomposites: effects of nano concentration and cation exchange. J Radioanal Nucl Chem 300:1217–1225
13. Anirudhan TS, Bringle CD, Rijith S (2010) Removal of uranium(VI) from aqueous solutions and nuclear industry effluents using humic acid-immobilized zirconium-pillared clay. J Environ Radioact 101:267–276
14. Bagherifam S, Lakzian A, Ahmadi SJ, Rahimi MF, Halajnia A (2010) Uranium removal from aqueous solutions by wood powder and wheat straw. J Radioanal Nucl Chem 283:289–296
15. Kütahyalı C, Eral M (2010) Sorption studies of uranium and thorium on activated carbon prepared from olive stones: kinetic and thermodynamic aspects. J Nucl Mater 396:251–256
16. Wang JS, Peng RT, Yang JH, Liu YC, Hu XJ (2011) Preparation of ethylenediamine-modified magnetic chitosan complex for adsorption of uranyl ions. Carbohyd Polym 84:1169–1175
17. Zareh MM, Aldaher A, Hussein AEM, Mahfouz MG, Soliman M (2013) Uranium adsorption from a liquid waste using thermally and chemically modified bentonite. J Radioanal Nucl Chem 295:1153–1159
18. Zhou LM, Wang YP, Liu ZR, Huang QW (2009) Characteristics of equilibrium, kinetics studies for adsorption of Hg(II), Cu(II), and Ni(II) ions by thiourea-modified magnetic chitosan microspheres. J Hazard Mater 161:995–1002
19. Wang Y, Gu ZX, Yang JJ, Liao JL, Yang YY, Liu N, Tang J (2014) Amidoxime-grafted multiwalled carbon nanotubes by plasma techniques for efficient removal of uranium(VI). Appl Surf Sci 320:10–20
20. Singh BN, Maiti B (2006) Seperation and preconcentration of U(VI) on XAD-4 modified with 8-hydroxy quinoline. Talanta 69:393–396
21. Kim JH, Lee HI, Yeon JW, Jung Y, Kim JM (2010) Removal of uranium(VI) from aqueous solutions by nanoporous carbon and

its chelating polymer composite. J Radioanal Nucl Chem 286:129–133
22. Özeroğlu C, Keçeli G (2009) Kinetic and thermodynamic studies on the adsorption of U(VI) ions on densely crosslinked poly(-methacrylic acid)from aqueous solutions. Radiochim Acta 97:709–717
23. Nogami M, Sugiyama Y, Kawasaki T, Harada M, Morita Y, Kikuchi T, Ikeda Y (2010) Adsorptivity of polyvinylpolypyrrolidone for selective separation of U(VI) from nitric acid media. J Radioanal Nucl Chem 283:541–546
24. Özeroğlu C, Metin N (2012) Adsorption of uranium ions by crosslinked polyester resin functionalized with acrylic acid from aqueous solutions. J Radioanal Nucl Chem 292:923–935
25. Chitrakar R, Tezuka S, Sonoda A, Sakane K, Ooi K, Hirotsu T (2006) Selective adsorption of phosphate from seawater and wastewater by amorphous zirconium hydroxide. J Colloid Interface Sci 297:426–433
26. Rodrigues LA, Maschio LJ, da Silva RE, da Silva MLCP (2010) Adsorption of Cr(VI) from aqueous solution by hydrous zirconium oxide. J Hazard Mater 173:630–636
27. Seredych M, Bandosz TJ (2011) Reactive adsorption of hydrogen sulfide on graphite oxide/$Zr(OH)_4$ composites. Chem Eng J 166:1032–1038
28. Dou XM, Mohan D, Pittman CU, Yang S (2012) Remediating fluoride from water using hydrous zirconium oxide. Chem Eng J 198–199:236–245
29. Peterson GW, Karwacki CJ, Feaver WB, Rossin JA (2009) Zirconium hydroxide as a reactive substrate for the removal of sulfur dioxide. Ind Eng Chem Res 48:1694–1698
30. Glover TG, Peterson GW, DeCoste JB, Browe MA (2012) Adsorption of ammonia by sulfuric acid treated zirconium hydroxide. Langmuir 28:10478–10487
31. Gao YY, Yuan YL, Ma DD, Li L, Li YH, Xu WH, Tao W (2014) Removal of aqueous uranyl ions by magnetic functionalized carboxymethylcellulose and adsorption property investigation. J Nucl Mater 453:82–90
32. Gupta VK, Jain CK, Ali I, Sharma M, Saini VK (2003) Removal of cadmium and nickel from wastewater using bagasse fly ash—a sugar industry waste. Water Res 37:4038–4044
33. Sureshkumar MK, Das D, Mallia MB, Gupta PC (2010) Adsorption of uranium from aqueous solution using chitosan-tripolyphosphate (CTPP) beads. J Hazard Mater 184:65–72
34. Mogilevsky G, Karwacki CJ, Peterson GW, Wagner GW (2011) Surface hydroxyl concentration on $Zr(OH)_4$ quantified by ^1H MAS NMR. Chem Phys Lett 511:384–388
35. Southon PD, Bartlett JR, Woolfrey JL, Ben-Nissan B (2002) Formation and characterization of an aqueous zirconium hydroxide colloid. Chem Mater 14:4313–4319
36. Elabd AA, Zidan WI, Abo-Aly MM, Bakier E, Attia MS (2014) Uranyl ions adsorption by novel metal hydroxides loaded Amberlite IR120. J Environ Radioact 134:99–108
37. Sun YB, Li JX, Wang XK (2014) The retention of uranium and europium onto sepiolite investigated by macroscopic, spectroscopic and modeling techniques. Geochim Cosmochim Ac 140:621–643
38. Sprynskyy M, Kovalchuk I, Buszewski B (2010) The separation of uranium ions by natural and modified diatomite from aqueous solution. J Hazard Mater 181:700–707
39. Fan FL, Qin Z, Bai J, Rong WD, Fan FY, Tian W, Wu XL, Wang Y, Zhao L (2012) Rapid removal of uranium from aqueous solutions using magnetic $Fe_3O_4@SiO_2$ composite particles. J Environ Radioact 106:40–46
40. Abbasizadeh S, Keshtkar AR, Mousavian MA (2014) Sorption of heavy metal ions from aqueous solution by a novel cast PVA/TiO_2 nanohybrid adsorbent functionalized with amine groups. J Ind Eng Chem 20:1656–1664
41. Qian LP, Ma MH, Cheng DH (2015) Adsorption and desorption of uranium on nano goethite and nano alumina. J Radioanal Nucl Chem 303:161–170
42. Hu R, Shao DD, Wang XK (2014) Graphene oxide/polypyrrole composites for highly selective enrichment of U(VI) from aqueous solutions. Polym Chem 5:6207–6215
43. Zhao YG, Li JX, Zhao LP, Zhang SW, Huang YS, Wu XL, Wang XK (2014) Synthesis of amidoxime-functionalized $Fe_3O_4@SiO_2$ core–shell magnetic microspheres for highly efficient sorption of U(VI). Chem Eng J 235:275–283
44. Song WC, Shao DD, Lu SS, Wang XK (2014) Simultaneous removal of uranium and humic acid by cyclodextrin modified graphene oxide nanosheets. Sci China Chem 57:1291–1299
45. Sun YB, Yang SB, Chen Y, Ding CC, Cheng WC, Wang XK (2015) Adsorption and desorption of U(VI) on functionalized graphene oxides: a combined experimental and theoretical study. Environ Sci Technol 49:4255–4262
46. Wang XX, Zhang SW, Li JX, Xu JZ, Wang XK (2014) Fabrication of Fe/Fe_3C@porous carbon sheets from biomass and their application for simultaneous reduction and adsorption of uranium(VI) from solution. Inorg Chem Front 1:641–648
47. Shao DD, Li JX, Wang XK (2014) Poly(amidoxime)-reduced graphene oxide composites as adsorbents for the enrichment of uranium from seawater. Sci China Chem 57:1449–1458
48. Ortaboy S, Atun G (2014) Kinetics and equilibrium modeling of uranium(VI) sorption by bituminous shale from aqueous solution. Ann Nucl Energy 73:345–354
49. Ding DX, Fu PK, Li L, Xin X, Hu N, Li GY (2014) U(VI) ion adsorption thermodynamics and kinetics from aqueous solution onto raw sodium feldspar and acid-activated sodium feldspar. J Radioanal Nucl Chem 299:1903–1909
50. Liu MX, Dong FQ, Yan XY, Zeng WM, Hou LY, Pang XF (2010) Biosorption of uranium by *Saccharomyces cerevisiae* and surface interactions under culture conditions. Bioresour Technol 101:8573–8580